New local mass relation for isobaric analogue states and isospin-nonconserving forces

G. J. Fu,[1] Y. Y. Cheng,[2] Y. H. Zhang,[3,*] P. Zhang,[3,4] P. Shuai,[3] Y. M. Zhao,[5,6,†] and M. Wang[3]

[1]*School of Physics Science and Engineering, Tongji University, Shanghai 200092, China*
[2]*Department of Physics, East China Normal University, Shanghai 200241, China*
[3]*Key Laboratory of High Precision Nuclear Spectroscopy and Center for Nuclear Matter Science, Institute of Modern Physics, Chinese Academy of Sciences, Lanzhou 730000, China*
[4]*Graduate University of Chinese Academy of Sciences, Beijing 100049, China*
[5]*Shanghai Key Laboratory of Particle Physics and Cosmology, INPAC, School of Physics and Astronomy, Shanghai Jiao Tong University, Shanghai 200240, China*
[6]*IFSA Collaborative Innovation Center, Shanghai Jiao Tong University, Shanghai 200240, China*

(Received 21 June 2017; revised manuscript received 14 November 2017; published 28 February 2018)

In this paper a new local mass relation is constructed for isobaric analogue states of four relating neighboring nuclei. The standard deviation from a linear fit of experimental data is 20–70 keV. The systematics of the local mass relation is discussed in terms of an empirical Coulomb energy formula and the isobaric multiplet mass equation. The local relation for nuclei in the pf shell is studied in the framework of the microscopic shell model. The results demonstrate the key roles played by the Coulomb interaction and an effective isospin-nonconserving nucleon-nucleon interaction in our new mass relation.

DOI: 10.1103/PhysRevC.97.024339

I. INTRODUCTION

Nuclear mass (or alternatively nuclear binding energy) is of great importance in nuclear physics [1,2]. Nuclear mass measurements challenge various nuclear models and provide us with important information of nucleon-nucleon interactions, shell evolution, quantum phase transition, nucleon pairing, and nuclear clustering. Accurate mass measurements and theoretical predictions are key inputs for theoretical studies on the origin of heavy elements in nuclear astrophysics.

Great efforts have been devoted to describing and predicting nuclear masses across the nuclide chart. Here, we mention popular global mass models, such as the Duflo-Zuker model [3], the Skyrme-Hartree-Fock-Bogoliubov theory [4], the finite-range droplet model [5], and the improved Weizsäcker-Skyrme model [6], and accurate local mass relations, such as the famous Garvey-Kelson relations [7–11], the Audi-Wapstra extrapolations [12,13], and the local mass relations associated with proton-neutron interactions [14–17].

From another perspective, one achieves satisfactory mass predictions for atomic nuclei with mass number $A < 80$ based on the Coulomb displacement energies (CDE) [18–25], viz., the difference between the binding energies of mirror nuclei,

$$E_{\mathrm{CDE}}(A,T) = B(A,T_z = -T) - B(A,T_z = T),$$

where $B(A,T_z = -T)$ is the binding energy of the proton-rich nucleus and $B(A,T_z = T)$ is the binding energy of the neutron-rich nucleus. B is taken to be positive, and thus E_{CDE} is negative. Using the isobaric multiplet mass equation (IMME) [26], CDE is given by $2bT$, where b is a coefficient determined by a global fitting to the experimental CDE data at an accuracy of ∼100 keV [22] or calculated using the nuclear shell model at an accuracy of 30–40 keV for a very limited number of nuclei [18,22]. In Ref. [21] Cole used an empirical Coulomb energy formula to calculate CDE for nuclei in the $0d_{3/2}$ and $0f_{7/2}$ shells with a standard deviation $\leqslant$125 keV. In Refs. [23,24] CDE was obtained by the Skyrme Hartree-Fock calculation with consideration of an isospin-nonconserving (INC) interaction, and the calculation is able to reproduce the experimental CDE for all but the lightest nuclei with a root-mean-square deviation of ∼100 keV.

In this paper we construct a new local mass relation for isobaric analogue states of four neighboring nuclei. The accuracy of our new mass relation is 20–70 keV. This paper is organized into five sections. In Sec. II, we discuss a procedure of parametrization and error evaluation, and present the new local mass relation. In Sec. III, we study the local mass relation in terms of a Coulomb energy formula and the IMME. In Sec. IV, we study the local mass relation for nuclei in the pf shell in the framework of the shell model; the effects of the Coulomb interaction and INC interactions are discussed. In Sec. V, we summarize our results.

II. NEW LOCAL MASS RELATION

A. Parametrization and error evaluation

As we study nuclear masses, it is economic to begin with the procedure of parametrization and error evaluation. We denote experimental mass data of isobaric analogue states by M_i and experimental uncertainty by σ_i, where i is an abbreviation of proton number Z, mass number A, and isospin T; $i = 1,2,\ldots,n$, and n is the number of data. We denote a mass

*Corresponding author: yhzhang@impcas.ac.cn
†Corresponding author: ymzhao@sjtu.edu.cn

formula by $f_i = f(i; p_1, p_2, \ldots, p_t)$, where $p_1, p_2, \ldots, p_t$ are independent parameters to be fixed.

In this paper we use the weighted standard deviation (SD), i.e.,

$$\sigma_{\rm SD} = \sqrt{\frac{n}{n-t} \cdot \frac{\sum_i^n w_i (M_i - f_i)^2}{\sum_i^n w_i}}. \quad (1)$$

The weight, w_i, is defined by

$$w_i = \frac{1}{{\sigma_{\rm th}}^2 + {\sigma_i}^2}, \quad (2)$$

where $\sigma_{\rm th}$ is the model error, which represents the deviation of the present formula from "the exact theory". In Refs. [5,27] $\sigma_{\rm th}$ is obtained by decoupling the experimental uncertainty from variance using the maximum-likelihood estimation,

$${\sigma_{\rm th}}^2 = \frac{\sum_i^n {w_i}^2 [(M_i - f_i)^2 - {\sigma_i}^2]}{\sum_i^n {w_i}^2}. \quad (3)$$

By solving Eqs. (2) and (3) iteratively, we obtain w_i and $\sigma_{\rm th}$. Then we determine the parameters, $p_1, p_2, \ldots, p_t$, by minimizing the SD in Eq. (1), namely we solve the following equations:

$$\frac{\partial}{\partial p_j} \sum_i^n w_i (M_i - f_i)^2 = 0, \quad j = 1,2,\ldots,t. \quad (4)$$

After obtaining $p_1, p_2, \ldots, p_t$, we substituted them into Eq. (3) and solve Eqs. (2) and (3) again. The above steps are iterated until w_i, $\sigma_{\rm th}$, $\sigma_{\rm SD}$, and $p_1, p_2, \ldots, p_t$ are converged.

B. Local mass relation

We construct a new local mass relation for isobaric analogue states of four neighboring nuclei:

$$\begin{aligned}\varepsilon(Z,A,T_1,T_2) \equiv\ & B(Z,A,T_1) - B(Z-1,A,T_1) \\ & - B(Z,A+1,T_2) + B(Z-1,A+1,T_2) \\ =\ & -M(Z,A,T_1) + M(Z-1,A,T_1) \\ & + M(Z,A+1,T_2) - M(Z-1,A+1,T_2),\end{aligned} \quad (5)$$

where $B(Z,A,T_1)$ is binding energy of the $T = T_1$ isobaric analogue states in the nucleus with proton number Z and mass number A, and $M(Z,A,T_1)$ is the corresponding mass excess. For short we call the nucleus with proton number Z and mass number A as the "reference nucleus" in Eq. (5). Masses of $T = 1/2$ isobaric analogue states are ground-state masses, which are taken from the experimental data in the 2012 atomic mass evaluation table (AME2012) [13]. Masses of isobaric analogue states with $T \geqslant 1$ are taken from the 2014 evaluated isobaric analogue state database (IAS2014 for short) [28]. Since the AME2012 and IAS2014 databases were published, new mass measurements were performed for the ground states of ^{44}V, ^{46}Cr, ^{48}Mn, ^{50}Fe, ^{54}Ni, ^{79}Y, ^{81}Zr, ^{83}Nb, ^{52}Co, ^{56}Cu, ^{82}Zr, and ^{84}Nb at the HIRFL-CSR facility [29–32]. The adopted values are shown in Table I.

A schematic diagram of $\varepsilon(Z,A,T_1,T_2)$ is shown in Fig. 1. Let us exemplify this with a simple case [shown in Fig. 2(a)]:

TABLE I. New experimental data of ground-state mass excesses (in keV). Here, all the states of the odd-mass nuclei have $T = 1/2$, and all the states of the even-mass nuclei have $T = 1$. The label "*" means the mass was measured recently.

Nucleus	Mass excess
$^{44}V^g$	−23818(20)[a]
$^{46}Cr^g$	−29471(11)[b]
$^{48}Mn^g$	−29299(7)[b]
$^{50}Fe^g$	−34477(6)[b]
$^{54}Ni^g$	−39278(4)[b]
$^{79}Y^g$	−57818(79)[c]
$^{81}Zr^g$	−57460(94)[c]
$^{83}Nb^g$	−57556(151)[c]
$^{52}Co^g$	−34361(8)*[d]
$^{56}Cu^g$	−38643(15)*[a]
$^{82}Zr^g$	−63631(11)*[c]
$^{84}Nb^g$	−61219(13)*[c]

[a]Reference [29].
[b]Reference [30].
[c]Reference [31].
[d]Reference [32].

the reference nuclei of ε are odd-proton-even-neutron nuclei with $A - 2Z = N - Z = -1$, $T_1 = 1/2$, and $T_2 = 1$. In the right-hand side of Eq. (5), the first two terms represent the ground-state energy difference between the reference nucleus and its mirror nucleus, and the last two terms represent the $T = 1$ isobaric-analogue-state energy difference between the odd-odd $N = Z$ nucleus and its adjoining neutron-rich even-even nucleus with mass number $A + 1$. Because isobaric analogue states have almost identical structures, their nuclear mean fields must be very close to each other. Therefore the above procedure cancels charge-independent two-body interactions as well as nuclear mean-field contributions, thus

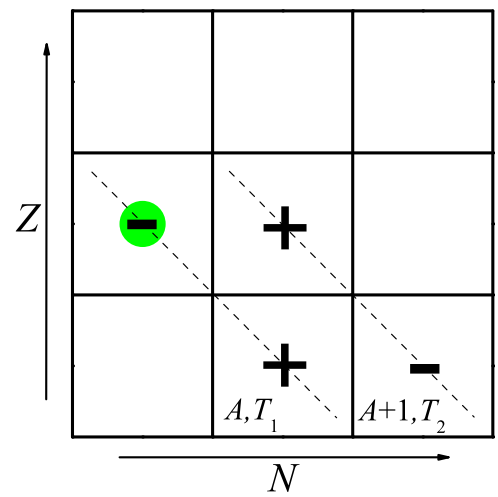

FIG. 1. The schematic diagram of the local mass relation, $\varepsilon(Z,A,T_1,T_2)$. The nucleus with solid circles in green is the reference nucleus which has proton number Z and mass number A. The plus and minus signs are consistent with those for mass excesses in Eq. (5).

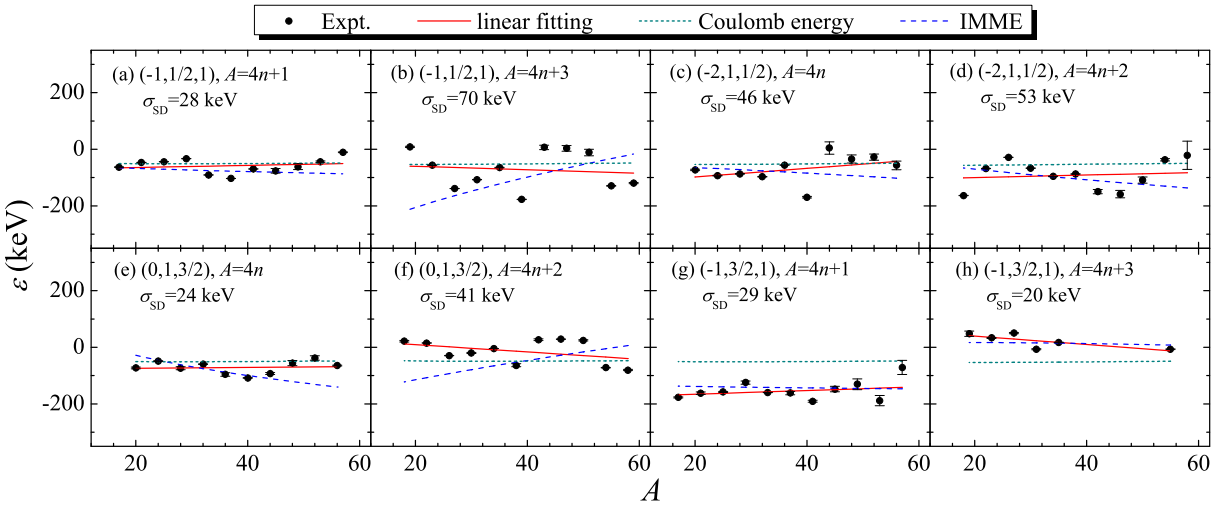

FIG. 2. ε derived from nuclear mass data in the AME2012, IAS2014, and Table I versus mass number A (with $A > 16$); the samples are separated into $4n$ groups. In each panel the values in the bracket are $(A-2Z, T_1, T_2)$. The solid curves in red are plotted using linear fitting (the standard deviations are denoted by $\sigma_{\rm SD}$); the dotted curves in green are plotted using the Coulomb energy formula; the dashed curves in blue are plotted using the IMME.

isolating the contribution of charge-violating interactions (e.g., the Coulomb energy). Absolute values of ε should be small. In Sec. III we shall show that ε can be approximately explained by the double difference of the Coulomb energies.

We show the results of ε for the following four cases: $(A-2Z, T_1, T_2) = (-1, 1/2, 1)$, $(-2, 1, 1/2)$, $(0, 1, 3/2)$, and $(-1, 3/2, 1)$. Separating the reference nuclei into four groups: $A = 4n$, $4n+1$, $4n+2$, and $4n+3$ (it is also called "$4n$ groups"), we present ε versus mass number A (with $A > 16$) in Fig. 2. The absolute values of ε are smaller than 200 keV. Results of linear fittings and the corresponding SDs are also given in Fig. 2. One sees the SD in Figs. 2(a), 2(e), 2(g), and 2(h) are very small (<30 keV). Such high accuracy of the local mass realtion provides us with a powerful tool to predict unknown masses near the $N = Z$ line, especially for proton-rich nuclei.

III. MACROSCOPIC PROPERTIES

The Coulomb interaction plays a dominant role in the energy difference between isobaric analogue states. In order to understand the local mass relation, the empirical Coulomb energy formula is assumed [33]:

$$E_c(Z,A) = [a_1 Z^2 + a_2 Z^{4/3} + a_3(1-(-)^Z)]\frac{e^2}{R(A)}, \quad (6)$$

where $a_1 Z^2$ is the direct term; $a_2 Z^{4/3}$ is the exchange term; $a_3(1-(-)^Z)$ is the pairing term; a_1, a_2, and a_3 are parameters; $R(A)$ is the nuclear radius. In this paper we use the diffuseness modified root-mean-square radius equation [34],

$$R(A) = \sqrt{\frac{3}{5}\left[(r_0 A^{1/3})^2 + \frac{7}{3}\pi^2 a_0^2\right]} \quad (7)$$

with $r_0 = 1.15$ fm and $a_0 = 0.35$ fm.

We fit a_1, a_2, and a_3 to experimental data of Coulomb displacement energies (CDE). The procedure is as follows. Using atomic masses in the AME2012, IAS2014, and Table I, we obtain 103 CDE data. Assuming the CDE is produced by the Coulomb energy, we obtain

$$\begin{aligned} E_{\rm CDE} &\approx -E_c(Z,A) + E_c(A-Z,A) \\ &= -[a_1(Z^2-(A-Z)^2) + a_2(Z^{4/3}-(A-Z)^{4/3}) \\ &\quad + a_3((-)^{A-Z}-(-)^Z)]\frac{e^2}{R(A)}. \end{aligned} \quad (8)$$

The parameters a_1, a_2, and a_3 are used to fit the 103 CDE data using the above equation with the parametrization procedure discussed in Sec. II A. Taking $e^2 = 1.44$ fm MeV, we obtain $a_1 = 0.465$, $a_2 = -0.474$, and $a_3 = -0.104$ with an SD of 257 keV. We note that the magnitude of the exchange term in this paper is relatively larger than that in Ref. [33].

Substituting the Coulomb energy for the mass excess in Eq. (5), the local mass relation is given by the double difference of the Coulomb energies, i.e.,

$$\begin{aligned} \varepsilon(Z,A,T_1,T_2) \approx &-E_c(Z,A) + E_c(Z-1,A) \\ &+ E_c(Z,A+1) - E_c(Z-1,A+1). \end{aligned} \quad (9)$$

The right-hand side of the above equation is independent of isospins T_1 and T_2. The result of Eq. (9) is presented as dotted curves in green in Fig. 2. The double difference of the Coulomb energies has a very small value, and it approximately agrees with the data of ε. This means most of the Coulomb energies is canceled out in the local mass relation. The residual fluctuation can be further explained by microscopic shell-model calculations with isospin-nonconserving interactions as well as the Coulomb interaction (to be discussed in Sec. IV).

In Figs. 2(g) and 2(h) one sees a systematical odd-even staggering effect: the data of ε are systematically smaller than the double difference of the Coulomb energies in Fig. 2(g), and the opposite happens in Fig. 2(h). This effect coincides with the so-called $4n$-group odd-even staggering effect in the isobaric

multiplet mass equation (IMME). The IMME is defined by

$$M_{\rm IMME}(A,T,T_z) = a(A,T) + b(A,T)T_z + c(A,T){T_z}^2, \quad (10)$$

where $T_z \equiv A/2 - Z$, and the coefficients a, b, and c are interpreted as the isoscalar, isovector, and isotensor parts of the nuclear Hamiltonian. Substituting the IMME for the mass excess in Eq. (5), we have

$$\begin{aligned}\varepsilon(Z,A,T_1,T_2) \approx & -M_{\rm IMME}\left(A,T_1,\frac{A}{2}-Z\right) + M_{\rm IMME}\left(A,T_1,\frac{A}{2}-Z+1\right)\\ & + M_{\rm IMME}\left(A+1,T_2,\frac{A+1}{2}-Z\right) - M_{\rm IMME}\left(A+1,T_2,\frac{A+1}{2}-Z+1\right),\\ = & \, b(A,T_1) - b(A+1,T_2) + [c(A,T_1) - c(A+1,T_2)](A-2Z+1) - c(A+1,T_2). \end{aligned} \quad (11)$$

The isoscalar term is canceled out in the relation. The global formulas of the coefficients b and c are given by

$$\begin{aligned} b &= M_n - M_{^1\rm H} - 720 \times S_b \times (A-1)A^{-1/3} + C_b,\\ c &= 3 \times (260 \times S_c \times A^{-1/3} + C_c), \end{aligned} \quad (12)$$

where S_b, S_c, C_b, and C_c are parameters to be determined by fitting mass data of isobaric analogue states. The adopted values are shown in Tables 1 and 2 in Ref. [28]. It is important to note that S_b, S_c, C_b, and C_c are determined for the $4n$ groups, respectively, due to a well-pronounced odd-even staggering effect [28,35,36].

The result of Eq. (11) is presented as dashed curves in blue in Fig. 2. The prediction of the IMME agrees with the odd-even staggering in Figs. 2(g) and 2(h). However, the global trends of the IMME result is not very good, e.g., sizable deviations are observed in the cases of Figs. 2(b) and 2(f), due to the error ($\sim$100 keV) of the global formula for the coefficient b [22,28].

IV. SHELL MODEL CALCULATION

In last section, we have studied the local mass relation in terms of the IMME, which does not discriminate between the Coulomb interaction and isospin-nonconserving (INC) interactions. In this section, we study the mass relation microscopically. For nuclei in the pf shell, this is carried out by the nuclear shell model with the KB3G interaction [37], the Coulomb interaction, and INC interactions. The IMME coefficients b and c are also studied through the same procedure.

The modern effective Coulomb interaction, $V_{\rm Coul}$, used in the shell-model calculation for nuclei in the pf shell contains three dominant terms [38]:

(a) The first term is Coulomb matrix elements obtained in the spherical harmonic oscillator basis.

(b) The second term is a monopole correction of the Coulomb energy due to the change of nuclear radius and/or deformation, whose contribution to the energy difference between isobaric analogue states is approximately proportional to the average proton plus neutron occupancies in the $1p_{3/2}$ orbit (denoted by $\langle m_{1p_{3/2}}\rangle$) [38,39]:

$$\begin{aligned}\Delta E_{\rm Cm} &= E_{\rm Cm}(Z,A) - E_{\rm Cm}(Z-1,A)\\ &\approx -\frac{(Z-1)}{20}\left(\frac{41}{A}\right)^{1/3}\alpha_r\langle m_{1p_{3/2}}\rangle, \end{aligned}$$

where α_r is a parameter, and $(\frac{41}{A})^{1/3}$ is a mass-dependent factor. In Refs. [39–41] one sets $\alpha_r = 300 \sim 400$ keV; in this work we set $\alpha_r = 300$ keV. It should be noticed that $\Delta E_{\rm Cm}$ cannot be derived by modifying the single-particle energy in the shell-model calculation.

(c) The third term consists of two single-particle corrections: one is the energy correction of the proton orbits due to the monopole Coulomb interaction in the core, which varies with the square of the orbital momentum $\boldsymbol{l}^2$ [40,42]; the other is the relativistic electromagnetic spin-orbit splitting, which is described using the Larmor-Thomas precession [33,43]. See Eq. (22) and Table 3 in Ref. [38] for the formulas.

Although the effective Coulomb interaction plays an important role in energy differences between isobaric analogue states, shell-model calculations provide inaccurate results. Thus INC nucleon-nucleon interactions are indispensable. An INC nucleon-nucleon interaction generally contains two terms: an isovector term $V^{(1)}_{\rm INC}$ and an isotensor term $V^{(2)}_{\rm INC}$. Assuming that $0f_{7/2}$ configurations are dominant in the nuclear wave functions, the INC interaction in the $0f_{7/2}$ orbit can be obtained:

(a) The isovector term of the INC interaction is defined by

$$\begin{aligned} V^{(1)}_{\rm INC} &= \sum_{Jm}\frac{\beta^{(1)}_J}{2}\left({A^J_{m,\pi\pi}}^\dagger A^J_{m,\pi\pi} - {A^J_{m,\nu\nu}}^\dagger A^J_{m,\nu\nu}\right),\\ {A^J_{m,\pi\pi}}^\dagger &= \frac{1}{\sqrt{2}}\left({a_{\pi 0f_{7/2}}}^\dagger \times {a_{\pi 0f_{7/2}}}^\dagger\right)^J_m,\\ {A^J_{m,\nu\nu}}^\dagger &= \frac{1}{\sqrt{2}}\left({a_{\nu 0f_{7/2}}}^\dagger \times {a_{\nu 0f_{7/2}}}^\dagger\right)^J_m, \end{aligned}$$

where $\beta^{(1)}_J$ are the two-body matrix elements. $V^{(1)}_{\rm INC}$ makes a significant contribution to mirror-excitation-energy differences. In Ref. [44] $\beta^{(1)}_J$ are optimized by fitting mirror-excitation-energy differences of yrast states for nuclei in the pf shell with $A = 42-54$, after considering the effective Coulomb interaction. We simply adopt those values.

(b) For the isotensor term of the INC interaction, we take a schematic form given in Ref. [40]:

$$\begin{aligned} V^{(2)}_{\rm INC} &= \frac{\beta^{(2)}_{J=0}}{6}\left({A^{J=0}_{\pi\pi}}^\dagger A^{J=0}_{\pi\pi} + {A^{J=0}_{\nu\nu}}^\dagger A^{J=0}_{\nu\nu} - 2{A^{J=0}_{\pi\nu}}^\dagger A^{J=0}_{\pi\nu}\right),\\ {A^{J=0}_{\pi\nu}}^\dagger &= \left({a_{\pi 0f_{7/2}}}^\dagger \times {a_{\nu 0f_{7/2}}}^\dagger\right)^{J=0}, \end{aligned}$$

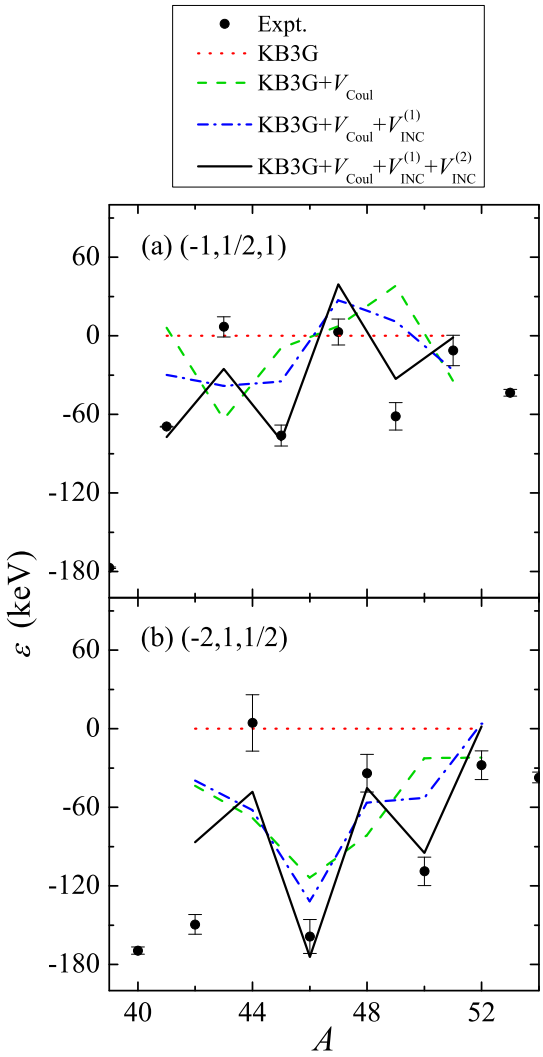

FIG. 3. The local mass relation ε calculated by the shell model with effective interactions for nuclei in the pf shell. The values in the brackets are $(A-2Z,T_1,T_2)$. $V_{\rm Coul}$ is the effective Coulomb interaction. $V^{(1)}_{\rm INC}$ and $V^{(2)}_{\rm INC}$ are the isovector and isotensor terms of the INC interaction, respectively.

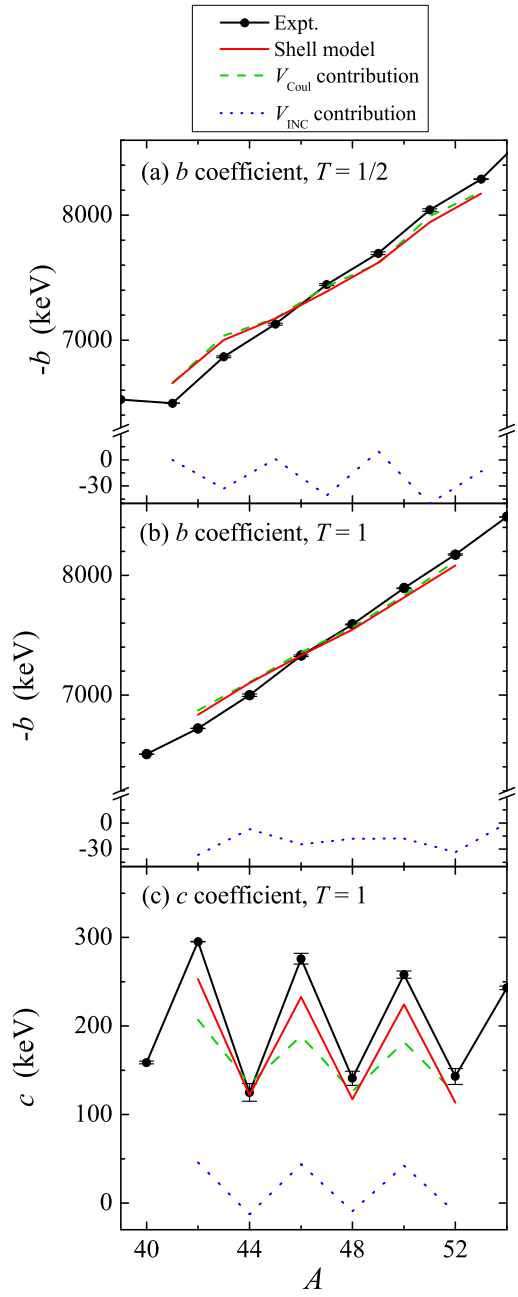

FIG. 4. IMME coefficients b and c for nuclei in the pf shell. In (a) and (b) the coefficient b is presented for $T=1/2$ and $T=1$ isobaric analogue states, respectively; in (c) the coefficient c is presented for $T=1$ isobaric analogue states. The shell-model results are obtained using the KB3G interaction, the Coulomb interaction, and the INC interaction.

where the two-body matrix element $\beta^{(2)}_{J=0}=100\,\text{keV}$. $V^{(2)}_{\rm INC}$ makes a significant contribution to triplet-excitation-energy differences between isobaric analogue states. In Refs. [40,44], $V^{(1)}_{\rm INC}$ and $V^{(2)}_{\rm INC}$ were optimized to describe excitation-energy differences. Here, we show that they also present good agreement with the local mass relation.

We study the local mass relation for the reference nuclei in the pf shell with $41\leqslant A\leqslant 52$, for two cases: $(A-2Z,T_1,T_2)=(-1,1/2,1)$ and $(-2,1,1/2)$. ε is derived using Eq. (5) in which the isobaric-analogue-state energies are calculated by the shell model. The NushellX shell-model code is used [45], with the KB3G interaction [37], $V_{\rm Coul}$, $V^{(1)}_{\rm INC}$, and $V^{(2)}_{\rm INC}$. The level energies are obtained by diagonalizing the Hamiltonians.

In Fig. 3 one sees ε obtained by the shell model with the original KB3G interaction is equal to zero, since there is no energy difference between isobaric analogue states under an isospin-conserving Hamiltonian. The Coulomb and INC interactions induce nonzero ε values.

For the case of $(A-2Z,T_1,T_2)=(-1,1/2,1)$ in Fig. 3(a), one sees that the experimental data of ε show a local odd-even staggering behavior, i.e., ε for the reference nuclei with $A=43,47,51$ are larger than those with $A=41,45,49$. Similarly, for the case of $(-2,1,1/2)$ in Fig. 3(b), the experimental

data of ε for the reference nuclei with $A = 44,48,52$ are larger than those with $A = 42,46,50$. The average value of ε calculated with the effective Coulomb interaction is close to the average value of the experimental data, but the local odd-even staggering behaviors are not reproduced by the Coulomb interaction. Considering the isovector and isotensor INC interactions, the resulting ε are in good agreement with the experimental data.

We study the IMME coefficients b and c [see Eq. (10)] for nuclei in the pf shell with $41 \leqslant A \leqslant 53$, using the shell model. It could be conjectured by intuition that the isovector part of the Coulomb interaction and the isovector INC interaction might be responsible for the coefficient b, and that the isotensor part of the Coulomb interaction and the isotensor INC interaction might be responsible for the coefficient c. In Fig. 4 one sees b and c obtained by the shell model are close to those derived by the experimental mass data. The dominant contribution to b and c comes from the Coulomb interaction. The odd-even staggering effect is found in the coefficient b for the $T = 1/2$ isobaric analogue states [see Fig. 4(a)] and in the coefficient c for the $T = 1$ isobaric analogue states [see Fig. 4(c)]. Both the Coulomb interaction and the INC interaction contribute to this odd-even staggering behavior. This result can be understood as a nuclear pairing effect [46], which is as follows. Due to the strong charge-independent pairing interaction, the $J = 0$ pair correlation is very strong in wave functions of low-lying states. The two-body matrix elements with $J = 0$, for both the Coulomb and INC interactions, have the largest absolute values, and thus the energy shift caused by these two interactions exhibits an odd-even staggering behavior.

V. SUMMARY

In this paper, we propose a new local mass relation, $\varepsilon(Z,A,T_1,T_2)$, for isobaric analogue states between four neighboring nuclei. We find remarkably good systematics of the local mass relation. The standard deviation from a linear fit through the data points is 20–70 keV. This accurate relation provides a new approach to predict nuclear masses with N close to Z.

We study ε in terms of an empirical Coulomb energy formula and the isobaric multiplet mass equation (IMME). The double difference of the Coulomb energies between four neighboring nuclei has a very small value, and it approximately agrees with the experimental data of ε. This means that in the local mass relation, it cancels mean-field energies, charge-independent two-body interactions, and most of the Coulomb energy. The residual fluctuation is due to microscopic quantum effects of charge-violating interactions. For the case of $(A-2Z,T_1,T_2) = (-1,3/2,1)$, there is an odd-even staggering effect: ε for the reference nuclei with $A = 4n+1$ is systematically smaller than that with $A = 4n+3$. The empirical Coulomb energy formula cannot explain this effect. We find the odd-even staggering of ε coincides with the so-called $4n$-group odd-even staggering in the IMME coefficients.

We have investigated ε for nuclei in the pf shell with $41 \leqslant A \leqslant 52$, in the framework of the microscopic shell model with the KB3G interaction, the effective Coulomb interaction, and an effective INC interaction. The effective INC interaction in the shell model was used to explain the excitation-energy differences between isobaric analogue states [44]. In this work we show that the effective INC interaction also presents good agreement with the mass (binding-energy) differences. Our results show that both the isovector and isotensor terms of the INC interaction, as well as the Coulomb interaction, are required to reproduce the local mass relation. We study the IMME coefficients b and c through the same procedure. The dominant contribution to b and c comes from the Coulomb interaction, and both the Coulomb interaction and the INC interaction contribute to the odd-even staggering of the IMME coefficients (due to a pairing effect), which leads to the odd-even staggering of ε.

It is worth noting that as one approaches the drip lines, where weakly bound states or resonance states may come in, coupling to continuum might disrupt the accuracy of this local mass relation.

ACKNOWLEDGMENTS

This work is supported by the Major State Basic Research Development Program of China (Grant No. 2013CB834401), the National Natural Science Foundation of China (Grant Nos. 11605122, 11505113, and 11675101), the Key Research Program of Frontier Sciences, CAS (Grant No. QYZDJ-SSW-S), the National Key Program for S&T Research and Development (Grant No. 2016YFA0400504), the Program of Shanghai Academic Research Leader (Grant No. 16XD1401600), Shanghai Key Laboratory of Particle Physics and Cosmology (Grant No. 15DZ2272100), and the Fundamental Research Funds for the Central Universities (Grant No. 2016KJ002). We thank Dr. Cenxi Yuan for useful discussion, and thank Dr. Yang Lei and Dr. Cenxi Yuan for double checking the shell-model results.

[1] D. Lunney, J. M. Pearson, and C. Thibault, Rev. Mod. Phys. **75**, 1021 (2003).
[2] K. Blaum, Phys. Rep. **425**, 1 (2006).
[3] J. Duflo and A. P. Zuker, Phys. Rev. C **52**, R23 (1995).
[4] S. Goriely, M. Samyn, and J. M. Pearson, Phys. Rev. C **75**, 064312 (2007); S. Goriely, N. Chamel, and J. M. Pearson, Phys. Rev. Lett. **102**, 152503 (2009).
[5] P. Möller, J. R. Nix, W. D. Myers, and W. J. Swiatecki, At. Data Nucl. Data Tables **59**, 185 (1995); P. Möller, W. D. Myers, H. Sagawa, and S. Yoshida, Phys. Rev. Lett. **108**, 052501 (2012).
[6] N. Wang, M. Liu, and X. Z. Wu, Phys. Rev. C **81**, 044322 (2010); M. Liu, N. Wang, Y. Deng, and X. Wu, *ibid.* **84**, 014333 (2011).
[7] G. T. Garvey and I. Kelson, Phys. Rev. Lett. **16**, 197 (1966); G. T. Garvey, W. J. Gerace, R. L. Jaffe, I. Talmi, and I. Kelson, Rev. Mod. Phys. **41**, S1 (1969).
[8] J. Jänecke and H. Behrens, Phys. Rev. C **9**, 1276 (1974); J. Jänecke, At. Data Nucl. Data Tables **17**, 455 (1976).
[9] J. Barea, A. Frank, J. G. Hirsch, and P. Van Isacker, Phys. Rev. Lett. **94**, 102501 (2005); J. Barea, A. Frank, J. G. Hirsch,

P. Van Isacker, S. Pittel, and V. Velázquez, Phys. Rev. C **77**, 041304(R) (2008); J. G. Hirsch, I. Morales, J. Mendoza-Temis, A. Frank, J. C. Lopez-Vieyra, J. Barea, S. Pittel, P. Van Isacker, and V. Velázquez, Int. J. Mod. Phys. E **17**, 398 (2008).

[10] Y. Y. Cheng, Y. M. Zhao, and A. Arima, Phys. Rev. C **89**, 061304(R) (2014).

[11] J. L. Tian, N. Wang, C. Li, and J. J. Li, Phys. Rev. C **87**, 014313 (2013).

[12] G. Audi, A. H. Wapstra, and C. Thibault, Nucl. Phys. A **729**, 337 (2003).

[13] M. Wang, G. Audi, A. H. Wapstra, F. G. Kondev, M. MacCormick, X. Xu, and B. Pfeiffer, Chin. Phys. C **36**, 1603 (2012).

[14] D. S. Brenner, C. Wesselborg, R. F. Casten, D. D. Warner, and J. Y. Zhang, Phys. Lett. B **243**, 1 (1990).

[15] P. Van Isacker, D. D. Warner, and D. S. Brenner, Phys. Rev. Lett. **74**, 4607 (1995).

[16] R. B. Cakirli, D. S. Brenner, R. F. Casten, and E. A. Millman, Phys. Rev. Lett. **94**, 092501 (2005); R. B. Cakirli and R. F. Casten, *ibid.* **96**, 132501 (2006); M. Stoitsov, R. B. Cakirli, R. F. Casten, W. Nazarewicz, and W. Satula, *ibid.* **98**, 132502 (2007).

[17] G. J. Fu, H. Jiang, Y. M. Zhao, S. Pittel, and A. Arima, Phys. Rev. C **82**, 034304 (2010); H. Jiang, G. J. Fu, Y. M. Zhao, and A. Arima, *ibid.* **82**, 054317 (2010); G. J. Fu, Y. Lei, H. Jiang, Y. M. Zhao, B. Sun, and A. Arima, *ibid.* **84**, 034311 (2011); H. Jiang, G. J. Fu, B. Sun, M. Liu, N. Wang, M. Wang, Y. G. Ma, C. J. Lin, Y. M. Zhao, Y. H. Zhang, Zhongzhou Ren, and A. Arima, *ibid.* **85**, 054303 (2012).

[18] W. E. Ormand and B. A. Brown, Nucl. Phys. A **491**, 1 (1989).

[19] B. A. Brown, Phys. Rev. C **43**, R1513 (1991).

[20] W. E. Ormand, Phys. Rev. C **53**, 214 (1996).

[21] B. J. Cole, Phys. Rev. C **54**, 1240 (1996).

[22] W. E. Ormand, Phys. Rev. C **55**, 2407 (1997).

[23] B. A. Brown, W. A. Richter, and R. Lindsay, Phys. Lett. B **483**, 49 (2000).

[24] B. A. Brown, R. R. C. Clement, H. Schatz, A. Volya, and W. A. Richter, Phys. Rev. C **65**, 045802 (2002).

[25] M. Bao, Y. Lu, Y. M. Zhao, and A. Arima, Phys. Rev. C **94**, 044323 (2016).

[26] E. P. Wigner, in *Proceedings of the R. A. Welch Foundation Conference on Chemical Research, Houston*, edited by W. O. Milligan (R. A. Welch Foundation, Houston, 1957), Vol. 1.

[27] P. Möller, J. R. Nix, W. D. Myers, and W. J. Swiatecki, At. Data Nucl. Data Tables **39**, 213 (1988).

[28] M. MacCormick and G. Audi, Nucl. Phys. A **925**, 61 (2014).

[29] Y. H. Zhang *et al.* (unpublished).

[30] P. Zhang *et al.*, Phys. Lett. B **767**, 20 (2017).

[31] Y. M. Xing *et al.* (unpublished).

[32] X. Xu, P. Zhang, P. Shuai, R. J. Chen, X. L. Yan, Y. H. Zhang, M. Wang, Y. A. Litvinov, H. S. Xu, T. Bao, X. C. Chen, H. Chen, C. Y. Fu, S. Kubono, Y. H. Lam, D. W. Liu, R. S. Mao, X. W. Ma, M. Z. Sun, X. L. Tu, Y. M. Xing, J. C. Yang, Y. J. Yuan, Q. Zeng, X. Zhou, X. H. Zhou, W. L. Zhan, S. Litvinov, K. Blaum, G. Audi, T. Uesaka, Y. Yamaguchi, T. Yamaguchi, A. Ozawa, B. H. Sun, Y. Sun, A. C. Dai, and F. R. Xu, Phys. Rev. Lett. **117**, 182503 (2016).

[33] J. A. Nolen and J. P. Schiffer, Annu. Rev. Nucl. Sci. **19**, 471 (1969).

[34] B. A. Brown, Lecture Notes in Nuclear Structure Physics, 2005, https://people.nscl.msu.edu/∼brown/Jina-workshop/BAB-lecture-notes.pdf/.

[35] J. Jänecke, Phys. Rev. **147**, 735 (1966).

[36] Y. H. Lam, N. A. Smirnova, and E. Caurier, Phys. Rev. C **87**, 054304 (2013).

[37] A. Poves, J. Sánchez-Solano, E. Caurier, and F. Nowacki, Nucl. Phys. A **694**, 157 (2001).

[38] M. A. Bentley and S. M. Lenzi, Prog. Part. Nucl. Phys. **59**, 497 (2007).

[39] A. P. Zuker, J. Duflo, S. M. Lenzi, G. Martínez-Pinedo, A. Poves, and J. Sánchez-Solano, arXiv:nucl-th/0104048.

[40] A. P. Zuker, S. M. Lenzi, G. Martínez-Pinedo, and A. Poves, Phys. Rev. Lett. **89**, 142502 (2002).

[41] S. M. Lenzi *et al.*, Phys. Rev. Lett. **87**, 122501 (2001).

[42] J. Duflo and A. P. Zuker, Phys. Rev. C **66**, 051304(R) (2002).

[43] D. R. Inglis, Phys. Rev. **50**, 783 (1936); **82**, 181 (1951).

[44] M. A. Bentley, S. M. Lenzi, S. A. Simpson, and C. Aa. Diget, Phys. Rev. C **92**, 024310 (2015).

[45] W. D. M. Rae, NUSHELLX code, http://www.garsington.eclipse.co.uk/.

[46] B. C. Carlson and I. Talmi, Phys. Rev. **96**, 436 (1954).